

Assessment of left ventricular function during upright treadmill exercise with tantalum 178 and multiwire gamma camera

Jaekyeong Heo, MD, FACC,^a Thein Htay, MD,^a Deval Mehta, MD,^a Liang Sun, PhD,^b Jeffrey Lacy, PhD,^b and Ami E. Iskandrian, MD, FACC^a

Background. Prior studies with first-pass radionuclide angiography (RNA) during treadmill exercise used a single-crystal (Anger) or multicrystal gamma camera and technetium 99m tracers. Motion correction, when done, used point sources, which limited correction to only plane movement.

Methods and Results. We examined the performance of a multiwire gamma camera (MWGC), generator-produced tantalum 178, and a novel method of motion correction during treadmill exercise testing. We studied 100 patients in whom rest and stress gated tomographic myocardial perfusion images were obtained. Eight patients were excluded because of incomplete data. There were 53 men and 39 women aged 52 ± 12 years. The resting left ventricular (LV) ejection fraction (EF) was $61\% \pm 12\%$ by gated single photon emission computed tomography. Stress myocardial perfusion was normal in 83 patients and abnormal in 9 patients. The resting RNA EF in the upright position was $57\% \pm 12\%$ ($r = 0.52$, $P = .0001$ vs gated EF). At peak exercise, the EF by MWGC was $60\% \pm 26\%$ if uncorrected and $69\% \pm 13\%$ after motion correction. Among the 80 patients with normal perfusion and normal resting EF by gated single photon emission computed tomography, a normal response to exercise was seen in 52 (63%) without motion correction and 74 (89%) with motion correction ($P < .05$).

Conclusion. Assessment of LV function is feasible with MWGC. The motion-corrected images significantly improved the results. (J Nucl Cardiol 2005;12:560-6.)

Key Words: Left ventricular function • tantalum 178 • multiwire gamma camera • radionuclide angiography

Assessment of left ventricular (LV) function during exercise is useful in the detection and risk assessment of patients with coronary artery disease (CAD). Patients with an exercise LV ejection fraction (EF) of 60% or greater have an excellent prognosis with an annual event rate comparable to an age-matched normal population.¹⁻⁷ Most of these studies were performed with either first-pass or gated radionuclide angiography (RNA). First-pass RNA is challenging because of motion artifacts during exercise. Previous studies used an external point

source for correcting cardiac motion.⁸⁻¹⁰ The point source is typically 10 to 15 mCi americium 241 attached to the anterior chest wall. This technique limits the correction to only a single plane and assumes that the patient is rotationally fixed. In addition, in these previous studies technetium 99m was used as the tracer, which has an ideal energy level (140 keV) but a relatively long half-life of 6 hours and hence a relatively high radiation burden if multiple studies are done. Tantalum 178 is a generator-produced radio-tracer that has a short half-life of 9.3 minutes and a low energy (55-65 keV), resulting in a low radiation exposure that makes it ideal for serial imaging.¹¹⁻¹³ A specially designed multiwire gamma camera (MWGC) is used for image acquisition and processing. This camera technology has been described previously.¹⁴⁻¹⁷ In summary, the MWGC is a proportional counter detector, which consists of a pressurized gas chamber and 3 parallel wire planes. Ionization by radiation event is collected at the anode, where the charge is amplified by gas avalanches. Outer cathode lines are orthogonally positioned and attached to discrete delay-line grids. The position signal is obtained by measuring the time of delay between the occurrence and arrival of the event by use of high-speed

From the Division of Cardiovascular Disease, Department of Medicine, University of Alabama at Birmingham, Birmingham, Ala,^a and Proportional Technology Inc, Houston, Tex.

This study was supported by the US Department of Health and Human Services (National Institutes of Health, National Heart, Lung, and Blood Institute) Grant 5R44HL062135-03.

Received for publication Dec 1, 2004; final revision accepted April 1, 2005.

Reprint requests: Jaekyeong Heo, MD, Nuclear Cardiology Laboratory, University of Alabama at Birmingham, 313 THT, 1900 University Blvd, Birmingham, AL 35294-0006; jheo@uab.edu.

1071-3581/\$30.00

Copyright © 2005 by the American Society of Nuclear Cardiology.
doi:10.1016/j.nuclcard.2005.05.021

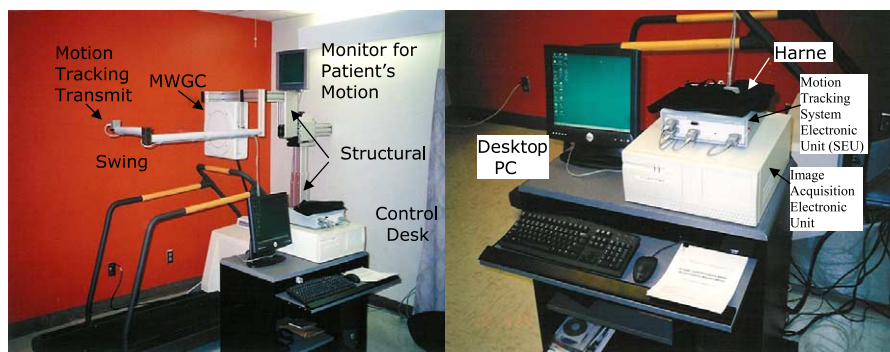


Figure 1. Setup of MWGC, motion-tracking device, and treadmill at the University of Alabama at Birmingham. The *left panel* shows the treadmill unit with the head of the MWGC attached to it. The motion-tracking transmitter is attached to a swinging arm. The monitor on top displays the position of the heart. The *right panel* shows two electronic units, one for motion tracking and the other for image acquisition.

delay-line readout system (mean clearance time, 150 nanoseconds). This enables digital recordings at very high rates (>1 million counts per second) and good image uniformity ($\pm 5\%$). The field of view of the MWGC is 25 cm in diameter. The intrinsic spatial resolution measured as full width at half maximum is 2.5 mm, and the system resolution at the camera surface is 6.9 mm with a high-sensitivity parallel-hole collimator.

The purposes of this study were to examine the feasibility of performing upright rest and peak exercise first-pass RNA and to examine the impact of a novel motion-correction algorithm on the EF responses to exercise in comparison to the results of single photon emission computed tomography (SPECT) perfusion imaging.

MATERIALS AND METHODS

Study Patients

We prospectively studied 100 patients who were referred for exercise SPECT perfusion imaging for clinical reasons. Each patient signed a consent form approved by the Institutional Review Board of the University of Alabama at Birmingham, Birmingham, Ala. Eight patients were excluded because of incomplete RNA data. There were 53 men and 39 women aged 52 ± 12 years. All patients underwent first-pass RNA at rest in the upright position. The patients then underwent symptom-limited treadmill exercise testing. Electrocardiography, blood pressure, and any symptoms were recorded throughout the exercise and recovery periods. Exercise was terminated as a result of excessive fatigue, marked ST changes, hypotension, syncope, severe angina, or severe arrhythmias. Just before peak exercise, repeat first-pass RNA was performed. The MWGC setup is shown in Figure 1. The rest and exercise studies were each obtained with a bolus injection of 15 to 40 mCi Ta-178 in the antecubital vein. Raw nuclear data at 120 frames per second and position data from the motion-tracking sensor were stored in the computer that is integrated in the

camera system. After injection of Ta-178, all patients, while exercising at peak exercise, were also injected with Tc-99m tetrofosmin for SPECT imaging and were asked to continue to exercise for 1 additional minute. The exercise RNA data were therefore obtained an average of 2 minutes before the termination of exercise.

Motion-Correction Algorithm

An electromagnetic position/orientation-tracking system (Polhemus Inc, Colchester, Vt) was used for motion correction and consists of a transmitter and a sensor. Excitation of the transmitter results in a sensor output that consists of 6-degree-of-freedom position information including joint-axial rotation. The motion-tracking system and motion-correction algorithm were tested with phantom studies simulating the conditions of treadmill RNA, and errors in position determination were less than the Nyquist spatial sampling rate (hence no image aliasing).¹⁸ Figure 2 shows the setup of the motion-tracking system, which keeps track of cardiac motion used in this study. Patients were asked to wear a special harness with a fixed motion-tracking sensor. The motion-tracking transmitter is attached to a swinging arm of the treadmill behind the patient's back. Before exercise, the chest contour of the patient is marked by use of another mobile sensor at 4 points in the same horizontal plane (8 cm below the sternal angle): the front, back, left, and right sides. This mobile sensor is used only at rest to determine the location of the heart, which is fed into the computer system, and the cardiac location is determined in relation to the fixed sensor attached to the harness (Figure 2). On the basis of the heart location in relation to the sensor (the motion-tracking sensor attached on the harness) and the instantaneous position of the sensor in the transmitter coordinates during exercise, the real-time heart location can be accurately tracked during the patient's movement on the treadmill.¹⁸

Special software was developed for real-time graphic display of the patient's heart position relative to the camera's field of view during the entire exercise period. Oftentimes, vigorous treadmill exercise can result in a loss of data because

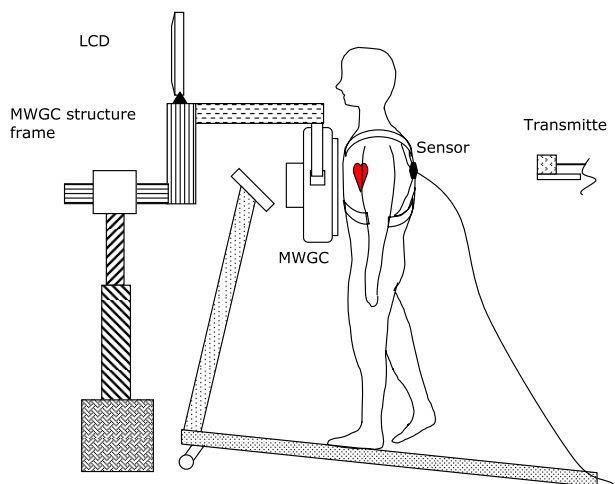


Figure 2. Schematic illustration of motion-tracking devices during exercise. By use of the transmitter and sensor, real-time position information is obtained.

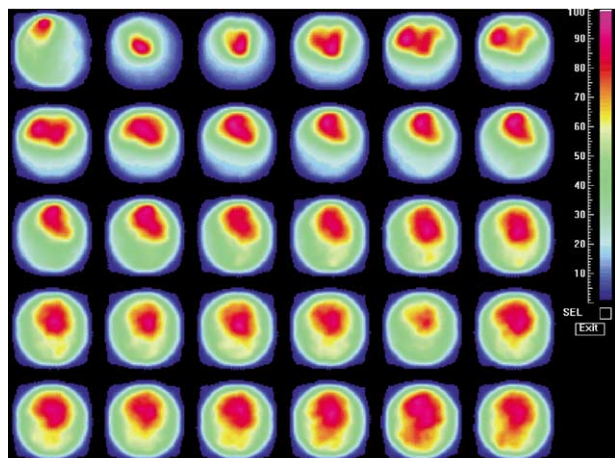


Figure 3. Serial 1-second images showing the bolus transit of tracer activity through the superior vena cava, right atrium, right ventricle, pulmonary artery, lungs, and left ventricle.

of a patient's lateral and vertical motion away from the camera's field. When the heart is moving out of the camera's field during exercise, the patient or technologist can immediately adjust so that the heart is always kept in the effective field of view of the camera.

After acquisition of first-pass RNA and motion data, images are corrected frame by frame for motion and saved for further analysis. Serial 1-second images are shown in Figure 3. After correction for dead time, background, and motion, images are reformatted as 40 frames per second and processed with analysis software. The first LV end-diastolic frame after the lung phase is selected, and the region of interest is drawn for the left ventricle (Figure 4). The software then constructs an activity histogram for the LV region and selects all ventricular beats (usually 4-6 beats) if their activity at end diastole is greater than 70% of the maximal LV activity at end diastole.

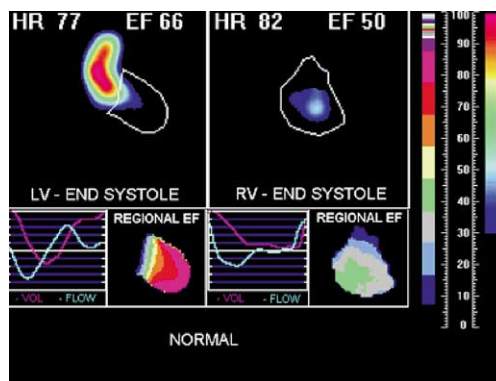


Figure 4. Region of interests drawn for LV and right ventricular (RV) functional analysis (resting study). HR, Heart rate.

The software finally combines the selected LV beats and applies lung background subtraction to form a single image sequence of a representative cardiac cycle, with a back-filling algorithm and spatial (2-4-2 convolution) filtering.¹⁵ LVEF was calculated as follows: $LVEF = (\text{End-diastolic counts} - \text{End-systolic counts}) / \text{End-diastolic counts} \times 100$.

Gated SPECT Perfusion Imaging

All patients underwent SPECT imaging via 1- or 2-day protocols with Tc-99m tetrofosmin as previously described.¹⁹⁻²¹ In brief, SPECT perfusion images were acquired with a dual-head gamma camera equipped with a low-energy, parallel-hole, high-resolution collimator (ADAC Laboratories, Milpitas, Calif). Stress images were obtained 30 to 60 minutes after tracer injection, and rest images were obtained at 60 to 90 minutes. An elliptical 180° anterior arc was used, starting at 45° right anterior oblique and ending at 45° left posterior oblique. Thirty-two projections were obtained for 20 to 40 seconds per projection with electrocardiographic gating at 8 frames per R-R cycle depending on the dose used. Filtered backprojection with a Butterworth filter was used for reconstruction. Because of the much lower energy of Ta-178 than Tc-99m, no appreciable spillover into the Tc-99m window was observed during perfusion image acquisition.

Statistical Analysis

All data are presented as mean ± SD. Statistical analysis was performed with SAS software (version 8.2; SAS Institute, Cary, NC).²² Categorical variables were assessed by the Pearson χ^2 test, and continuous variables were examined by use of the Student *t* test. Correlation was measured by use of the Pearson coefficient and Bland-Altman plots. A *P* value of < .05 was considered statistically significant.

RESULTS

The pertinent data in the 92 patients are shown in Table 1. There were 53 men and 39 women aged 52 ± 12

Table 1. Patient demographics (N = 92)

Age (y)	52 ± 12y
Men/women (n)	53/39
History of hypertension	35 (38%)
History of diabetes mellitus	77 (84%)
Atypical chest pain	61 (66%)
Resting electrocardiographic abnormalities	10 (11%)
Resting heart rate (beats/min)	75 ± 13
Exercise heart rate (beats/min)	144 ± 20
Resting systolic pressure (mm Hg)	127 ± 16
Exercise systolic pressure (mm Hg)	160 ± 80
Exercise time (min)	8.1 ± 2.6
Chest pain during exercise	2 (2%)
Positive ST changes	2 (2%)
Resting LVEF by gated SPECT (%)	61 ± 12
Resting LVEF by resting RNA (%)	57 ± 12
Uncorrected peak exercise LVEF (%)	60 ± 26
Corrected peak exercise LVEF (%)	69 ± 13

Values are given as mean ± SD or No. (%), unless otherwise indicated.

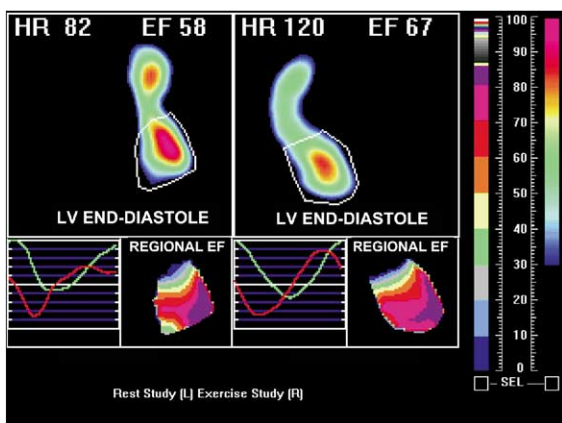


Figure 5. Representative examples of rest and corrected exercise RNA results. *HR*, Heart rate.

years. These patients had a low pretest probability of CAD and had presented with atypical chest pains or other symptoms. Only 2% had chest pain or ST depression during exercise. The rest and exercise SPECT perfusion images were normal in 83 patients; the remaining patients had ischemia (n = 4) or scar (n = 5). The gated SPECT LVEF was 61% ± 12%; it was normal (>45%) in 80 of 83 patients with normal perfusion. A representative example of rest and exercise RNA results is shown in Figure 5. The image quality was judged to be good or excellent in 95% of the RNA studies. A representative example of motion-corrected exercise RNA and uncorrected (raw) RNA results is shown in Figure 6. The RNA analysis on uncorrected images

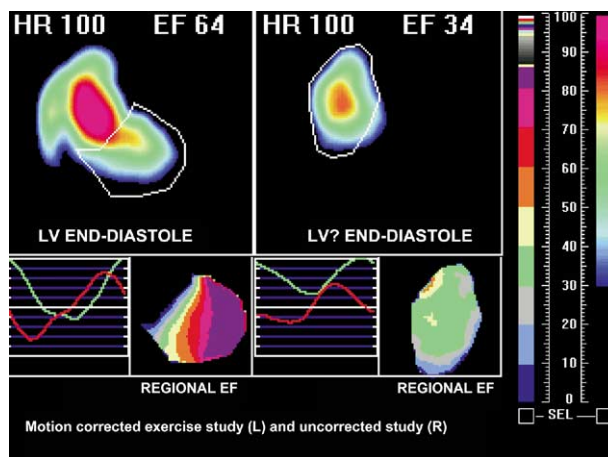


Figure 6. Representative examples of corrected and uncorrected exercise RNA results. *HR*, Heart rate.

results in incorrect definition of the end-diastolic LV region. The motion artifacts in tracer diffusion in sequential images related to the representative cardiac cycle cause the analysis software to make incorrect edge determinations, creating much-reduced LVEF values. The correlation and Bland-Altman plots between rest RNA EF and rest gated SPECT are shown in Figure 7. There was a statistically significant correlation between the two methods ($r = 0.52$; slope, 0.54; intercept, 23.9; standard error of the estimate [SEE], 9.0%; $P < .0001$). The changes in LVEF from rest to exercise with and without motion correction are shown in Figure 8.

The LVEF response to exercise was normal (>5% increase from rest to exercise) in 52 patients (63%) with normal SPECT images without motion correction and 74 (89%) with motion correction ($P < .05$). Of 6 patients with abnormal EF responses, 5 had hypertension.

DISCUSSION

A major strength of nuclear imaging is its ability to measure LVEF and right ventricular EF accurately and reproducibly. Unlike with other imaging methods such as 2-dimensional echocardiography, magnetic resonance imaging, and contrast angiography, the EF is measured by a count-based, non-geometric method.²³⁻²⁶ The assumption, which is valid, is that counts are proportional to volumes. Earlier planar (2-dimensional) methods were used in the form of first-pass or gated equilibrium RNA. The gated RNA (also known as MUGA [multigated acquisition]) was the most popular method because it could readily be performed with the standard Anger gamma camera. Both the first-pass and MUGA methods used Tc-99m tracers for image acquisition. More recently, a tomographic MUGA method has been evalu-

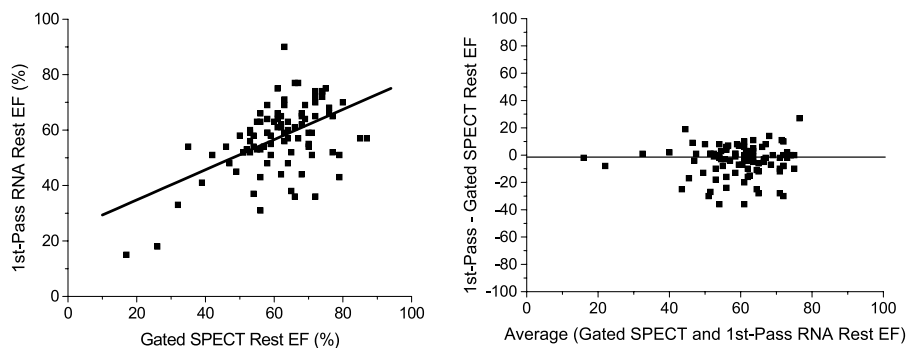


Figure 7. *Left panel*, Correlation between gated SPECT LVEF and rest RNA LVEF ($r = 0.52$, $P = .0001$). *Right panel*, Bland-Altman plot between the two values. The *x-axis* represents the average of two values, and the *y-axis* represents the differences.

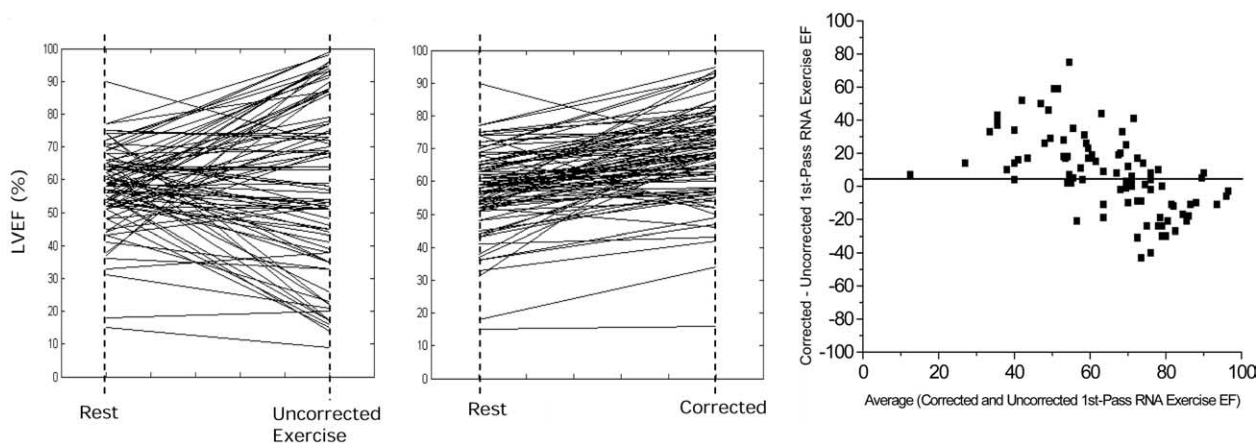


Figure 8. LVEF from rest to exercise without motion correction (*left panel*) and with motion correction (*middle panel*). *Right panel*, Bland-Altman plot showing relationship between the two values (with and without motion correction). The *x-axis* represents the average of two values, and the *y-axis* represents the differences.

ated to assess right ventricular and LV function.^{27,28} The tomographic (or SPECT) MUGA method allows 3-dimensional evaluation of LV regional and global functions, again with the use of Tc-99m. The SPECT MUGA method provides EF by either a count-based or a volume-based method, not unlike SPECT perfusion imaging.

Prior studies have shown that rest and exercise RNA results provide a wealth of information about the detection of CAD and prediction of future cardiac events. Exercise LVEF was found to be the single most important predictor of events (death or nonfatal myocardial infarction) in patients with known or suspected CAD and provided incremental prognostic information to other variables derived from clinical evaluation, exercise testing, and coronary angiography.^{29,30} In addition, the EF provides incremental prognostic information to perfusion imaging, as is done with gated SPECT perfusion imaging.^{31,32} The EF may be a stronger predictor of death, whereas ischemia, detected by perfusion imaging, may

be a stronger predictor of nonfatal myocardial infarction.^{33,34}

Over the past decade or longer, there has been a notable decline in the interest and number of exercise RNA studies, coupled with an exponential rise in the number of perfusion SPECT studies. Evaluation of rest and exercise RNA may, however, be appealing, as the method is less time-consuming and the tracer is less expensive. If these advantages are coupled with a less expensive gamma camera and better methods for motion correction, the method may become even more appealing at least in subgroups of patients such as those with a low pretest probability of CAD or to follow the effects of treatment in patients with a high pretest likelihood of CAD.

Most prior first-pass RNA studies used a multi-crystal gamma camera, which has a high count-rate capability. With advancement in single-crystal (Anger) gamma camera technology, its performance has

also improved. Nichols et al used motion correction with Am-241 to obtain first-pass RNA with both camera systems.⁸ Linear regression analysis of first-pass against MUGA EF demonstrated good correlation ($r = 0.92$; slope, 0.90; intercept, 3.8; SEE, 6.4%). First-pass EF by use of the Anger camera also correlated linearly with multicrystal camera values ($r = 0.94$; slope, 1.05; intercept, 1.3; SEE, 5.3%).

The MWGC unit used in this study has a good count-rate performance, better spatial resolution, and excellent field uniformity compared with a conventional multicrystal camera. The camera is the size of a 2-dimensional echocardiography machine, if not smaller, and hence is truly portable and mobile, permitting bedside measurements in the hospital including emergency departments, intensive care units, or cardiac catheterization laboratories. The onboard generator allows elution of Ta-178 onsite, and along with the short half-life of the tracer and the low radiation dose, serial measurements are possible. The tungsten 178/Ta-178 generator has a half-life of 22 days. Ta-178 decays to stable hafnium 178 by emitting x-rays with energies between 55 and 65 keV. It is estimated that the radiation dose from 10 RNA studies via Ta-178 is comparable to the exposure from a single MUGA or first-pass RNA study with Tc-99m.¹⁷ The built-in computer allows onsite processing of the entire study.

This study shows the feasibility of obtaining high-quality rest and peak exercise first-pass RNA by use of an integrated system of an MWGC, a tracer with a short half-life, and a novel method of motion correction that has never been previously used. This study shows that motion correction is important and EF data agreed with gated SPECT measurements. These LVEF data have a proven record of validity in patient care and risk assessment. The use of this method in subgroups of lower-risk patients will reduce the need for more expensive SPECT perfusion technology and will help reduce health costs and save time. In addition, the method may prove useful to identify high-risk patients and to follow-up such patients after therapeutic interventions. Further studies with this camera system are needed to test this hypothesis.

It should be noted that prior studies using first-pass RNA in risk assessment used bicycle exercise and no motion correction, whereas our study used treadmill exercise and motion correction. Further studies are needed to examine the prognostic value of the new method.

Acknowledgment

The authors have indicated they have no financial conflicts of interest.

References

1. Iskandrian AE, Verani M. Nuclear cardiac imaging: principles and applications. 3rd ed. New York: Oxford University Press; 2002.
2. Jones RH, Floyd RD, Austin EH, Sabiston DC Jr. The role of radionuclide angiography in the preoperative prediction of pain relief and prolonged survival following coronary artery bypass grafting. *Ann Surg* 1983;197:743-54.
3. Borer JS, Kent KM, Bacharach SL, Green MV, Rosing DR, Seides SF, et al. Sensitivity, specificity and predictive accuracy of radionuclide cineangiography during exercise in patients with coronary artery disease. Comparison with exercise electrocardiography. *Circulation* 1979;60:572-80.
4. Iskandrian AS, Hakki AH, Goel IP, Mundth ED, Kane-Marsch SA, Schenk CL. The use of rest and exercise radionuclide ventriculography in risk stratification in patients with suspected coronary artery disease. *Am Heart J* 1985;110:864-72.
5. Maniary DE, Kostuk WJ. Left and right ventricular function at rest and during bicycle exercise in the supine and sitting positions in normal subjects and patients with coronary artery disease. Assessment by radionuclide ventriculography. *Am J Cardiol* 1983;51:36-42.
6. Foster C, Pollock ML, Rod JL, Dymond DS, Wible G, Schmidt DH. Evaluation of functional capacity during exercise radionuclide angiography. *Cardiology* 1983;70:85-93.
7. Kazmers A, Cerqueira MD, Zierler RE. The role of preoperative radionuclide left ventricular ejection fraction for risk assessment in carotid surgery. *Arch Surg* 1988;123:416-9.
8. Nichols K, DePuey EG, Gooneratne N. First-pass ventricular ejection fraction using a single crystal nuclear camera. *J Nucl Med* 1994;35:1292-300.
9. Friedman JD, Berman DS, Kiat H, Bietendorf J, Hyun M, Van Train KF, et al. Rest and treadmill exercise first-pass radionuclide ventriculography: validation of left ventricular ejection fraction measurements. *J Nucl Med* 1995;36:1941-4.
10. Yano S, Tamaki N, Fujita T, Shirakawa S, Takahashi N, Kudoh T, et al. Motion correction in exercise first-pass radionuclide ventriculography without an external point source. *J Nucl Med* 1995;36:1941-4.
11. Holman BL, Neirinckx RD, Treves S, Towe DE. Cardiac imaging with tantalum-178. *Radiology* 1979;131:525-6.
12. Leblanc AD, Lacy JL, Johnson PC, Poliner LR, Jhingran SG. Tantalum-178 count-rate limitations of Anger and multicrystal cameras. *Radiology* 1983;46:242-3.
13. Lacy JL, Ball ME, Verani MS, Wiles HB, Babich JW, LeBlanc AD, et al. An improved tungsten-178/tantalum-178 generator system for high volume clinical applications. *J Nucl Med* 1988;29:1526-38.
14. Lacy JL, LeBlanc AD, Babich JW, Bungo MW, Latson LA, Lewis RM, et al. Gamma camera for medical applications using a multiwire proportional counter. *J Nucl Med* 1984;25:1003-12.
15. Verani MS, Lacy JL, Guidry GW, Nishimura S, Mahmarian JJ, Athanasoulis T, et al. Quantification of left ventricular performance during transient coronary occlusion at various anatomic sites in humans: a study using tantalum-178 and a multiwire gamma camera. *J Am Coll Cardiol* 1992;19:297-306.
16. Gioia G, Lin B, Katz R, DiMarino AJ, Ogilby JD, Cassel D, et al. Use of tantalum-178 generator and a multiwire gamma camera to study the effect of the Mueller maneuver on left ventricular performance: comparison to hemodynamics and single-photon emission computed tomography perfusion patterns. *Am Heart J* 1995;130:1062-7.

17. Lacy JL, Verani MS, Ball ME, Boyce TM, Gibson RW, Roberts R. First-pass radionuclide angiography using a multiwire gamma camera and tantalum. *J Nucl Med* 1988;29:293-301.
18. Sun L, Lacy JL, Martin CS, Nayak N, Clark JW. Implementation and performance of a motion tracking system for treadmill MWGC imaging studies. In: IEEE Nuclear Science Symposium Conference 2001 Record CD-ROM, ISBN 0-7803-7326-X. Proceedings of Medical Imaging Conference; San Diego, Calif; 2001.
19. Iskandrian AE, Heo J, Kong B, Lyons E, Marsch S. Use of technetium-99m isonitrite (RP-30a) in assessing left ventricular perfusion and function at rest and during exercise in coronary artery disease, and comparison with coronary arteriography and exercise thallium-201 SPECT imaging. *Am J Cardiol* 1989;64:270-5.
20. Go V, Bhatt MR, Hendel RC. The diagnostic and prognostic value of ECG-gated SPECT myocardial perfusion imaging. *J Nucl Med* 2004;45:912-21.
21. Patel AD, Abo-Auda WS, Davis JM, Zoghbi GJ, Deierhoi MH, Heo J, et al. Prognostic value of myocardial perfusion imaging in predicting outcome after renal transplantation. *Am J Cardiol* 2003;92:146-51.
22. SAS, version 8.2. Cary (NC): SAS Institute.
23. Van Dyke D, Anger HO, Sullivan RW, Vetter WR, Yano Y, Parker HG. Cardiac evaluation from radioisotope dynamics. *J Nucl Med* 1972;13:585-8.
24. Strauss HW, Zaret BL, Hurley PJ, Natarajan TK, Pitt B. A scintiphographic method for measuring left ventricular ejection fraction in man without cardiac catheterization. *Am J Cardiol* 1971;28:575-80.
25. Green MV, Bacharach SL, Borer JS, Bonow RO. A theoretical comparison of first-pass and gated equilibrium methods in the measurement of systolic left ventricular function. *J Nucl Med* 1991;32:1801-7.
26. Slutsky R, Gordon D, Karliner J, Battler A, Walaski S, Verba J, et al. Assessment of early ventricular systole by first-pass radionuclide angiography: useful method for detection of left ventricular dysfunction at rest in patients with coronary artery disease. *Am J Cardiol* 1979;44:459-62.
27. Nichols K, Humayun N, De Bondt P, Vandenberghe S, Akinboboye OO, Bergmann SR. Model dependence of gated blood pool SPECT ventricular function measurements. *J Nucl Cardiol* 2004;11:282-92.
28. Daou D, Van Krieking SD, Coaguila C, Lebtahi R, Fourme T, Sitbon O, et al. Automatic quantification of right ventricular function with gated blood pool SPECT. *J Nucl Cardiol* 2004;11:293-304.
29. Lee KL, Pryor DB, Pieper KS, Harrell FE Jr, Califf RM, Mark DB, et al. Prognostic value of radionuclide angiography in medically treated patients with coronary artery disease. A comparison with clinical and catheterization variables. *Circulation* 1990;82:1705-17.
30. Travin MI, Heller GV, Johnson LL, Katten D, Ahlberg AW, Isasi CR, et al. The prognostic value of ECG-gated SPECT imaging in patients undergoing stress Tc-99m sestamibi myocardial perfusion imaging. *J Nucl Cardiol* 2004;11:253-62.
31. Sharir T, Germano G, Kavanagh PB, Lai S, Cohen I, Lewin HC, et al. Incremental prognostic value of post-stress left ventricular ejection fraction and volume by gated myocardial perfusion single photon emission computed tomography. *Circulation* 1999;100:1035-42.
32. Hachamovitch R, Berman DS, Shaw LJ, Kiat H, Cohen I, Cabico JA, et al. Incremental prognostic value of myocardial perfusion single-photon emission computed tomography for the prediction of cardiac death. Differential stratification for risk of cardiac death and myocardial infarction. *Circulation* 1998;97:535-43.
33. Sharir T, Germano G, Kang X, Lewin HC, Miranda R, Cohen I, et al. Prediction of myocardial infarction versus cardiac death by gated myocardial perfusion SPECT: risk stratification by the amount of stress-induced ischemia and the poststress ejection fraction. *J Nucl Med* 2001;42:831-7.
34. Travin MI, Boucher CA, Newell JB, LaRaia PJ, Flores AR, Eagle KA. Variables associated with a poor prognosis in patients with an ischemic thallium-201 exercise test. *Am Heart J* 1993;125:335-44.